Rapid Communications

Axion production in unstable magnetized plasmas

J. T. Mendonça,[1,2] J. D. Rodrigues,[1,2,3] and H. Terças[1,2,*]

[1]*Instituto de Plasmas e Fusão Nuclear, Lisboa, Portugal*
[2]*Physics Department, Instituto Superior Técnico, Av. Rovisco Pais 1, 1049-001, Lisboa, Portugal*
[3]*Physics Department, Blackett Laboratory, Imperial College London, Prince Consort Road, SW7 2AZ, United Kingdom*

(Received 21 January 2019; revised manuscript received 15 April 2019; accepted 14 February 2020; published 17 March 2020)

Axions, the hypothetical particles restoring the charge-parity symmetry in the strong sector of the Standard Model and one of the most prone candidates for dark matter, are well known to interact with plasmas. In a recent publication [Phys. Rev. Lett. **120**, 181803 (2018)], we show that if the plasma dynamically responds to the presence of axions, then a new quasiparticle (the axion-plasmon polariton) can be formed, being at the basis of a new generation of plasma-based detection techniques. In this work, we exploit the axion-plasmon hybridization to actively produce axions in streaming magnetized plasmas. The produced axions can then be detected by reconversion into photons in a scheme that is similar to the light-shining-through-a-wall experiments.

DOI: 10.1103/PhysRevD.101.051701

I. INTRODUCTION

Axions and axionlike particles (ALPs) are hypothetical particles that have been proposed to solve the strong charge-parity (CP) problem [1–3]. At the origin of the latter, is the fact that nonperturbative (instanton) effects force the QCD Lagrangian to contain a total derivative with an arbitrary parameter (an angle θ) which does not vanish at infinity, therefore violating the CP symmetry. This is in blatant contradiction with the fact that strong interactions conserve CP [4]. Strong bounds on the neutron electric dipole moment imply that $\theta \lesssim 10^{-9}$ for the QCD to be compatible with the experiments [1]. A first, dynamical mechanism allowing $\theta \to 0$ was put forward by Peccei and Quinn [5], with the axion being later identified as the Goldstone boson associated with the spontaneous symmetry breaking of the continuous Peccei-Quinn $U(1)_{\mathrm{PQ}}$ symmetry [6,7].

Axions and ALPs are predicted to have an extremely small mass (possibly in the meV range) and couple very weakly to ordinary matter. For that reason, ALPs became appealing candidates (arguably, the most well theoretically motivated) to fix the dark matter puzzle as well [8,9]. Many facilities have been built with the goal of observing axion or ALP signatures, both based on laboratory and astrophysical observations [10–16]. However, given the smallness of the axion-photon coupling, testing the axion is difficult, rendering most of the experimental observations inconclusive. Telescope experiments, such as CAST—the most recent results establishing $g < 0.66 \times 10^{-10}$ GeV^{-1} for $m_\varphi < 0.02$ eV at the 2σ level [17]—and Asztalos *et al.* [18,19], the ADMX Collaboration [20], Vogel *et al.* [21], and MADMAX [22] investigating more precise regions of the QCD axion parameter space, are designed to probe axions produced by astrophysical objects. By construction, these experiments rely on a *passive* approach, in the sense that no axion production is envisaged. It is therefore desirable to look for alternatives, where axions could be *actively* produced in the lab. This motivation is at the basis of the "light-shining-through-a-wall" (LSW) strategy [23], such as those implemented by Bhre *et al.* [24] and OSQAR [25] using near infrared and visible light and Capparelli *et al.* [26] and Betz *et al.* [27] using sub-THz and microwave radiation.

One important limitation of the previous LSW schemes is the extremely low value of the axion-photon (and vice versa) conversion probabilities, a fact than can be somehow circumvented by allowing axion conversion to take place in a plasma [28]. Actually, there is recent hype around plasmas in the context of particle physics. The wakefield acceleration paradigm, for example, has gained much breath as it reveals to be an efficient way to accelerate particles [29–31], as recently demonstrated by the latest experiments by Adli *et al.* [32]. Interestingly, recent theoretical studies have pointed out that such wakefields could ultimately be used to produce ALPs in the lab [33–35] and that petawatt lasers could also do the job [36]. Plasmas are also playing a prominent role in axion astrophysics, as they have been put forward as vehicles for efficient axion-photon conversion in the atmosphere of magnetars [37–39]. Recently, a scheme based on a plasma metamaterial has been proposed to enhance the sensitivity of haloscopes [40].

In this Rapid Communication, we show that axions and axionlike particles can be actively produced in an unstable magnetized plasma, putting forward the physical principle for a "plasma-shinning-through-a-wall" (PSW)

*hugo.tercas@tecnico.ulisboa.pt

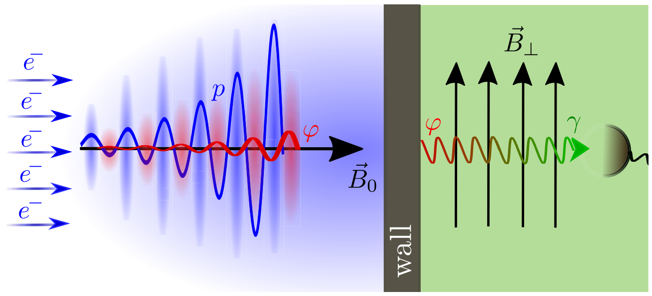

FIG. 1. Sketch of a "plasma-shining-a-wall" experiment based on the beam-plasma instability. A collimated electron beam (blue arrows) is injected into a cold plasma (blue shadow), leading to the growth of plasmons (p). The longitudinal magnetic field $\mathbf{B}_0$ then converts the plasmons into axions or ALPs (φ). The plasma and its radiation are blocked by a wall. The axions passing the wall are finally converted back into photons (γ) in the transverse magnetic field $\mathbf{B}_\perp$, being probed by a single-photon microwave detector.

strategy. If an energetic electron beam is injected in the plasma, unstable electron waves, or plasmons, are produced. This effect is dubbed in the literature as the beam-plasma instability [41,42]. The growing plasmon perturbation then provides the energy for the growth of axions. A schematic representation of the process is depicted in Fig. 1. In the absence of axions, the plasmons are insensitive to the magnetic field; however, if axions exist, they admix with the plasmons, leading to the formation of a hybrid quasiparticle, the axion-plasmon polariton [43]. As such, if the plasmons become dynamically unstable, their small axion component will also grow, leading to an efficient axion production in laboratory conditions. As a matter of fact, plasmon-axion mixing (differing from photon-axion mixing in plasmas) was first considered in Ref. [44], although no physical consequences were exploited there. Our estimates based on realistic experimental conditions show that a remarkably high plasmon-axion conversion probability can be achieved as a consequence of the beam-plasma instability. We predict a detectable photon signal for the axions passing the wall. Some implications of the radio signals emitted by pulsars are also discussed.

II. BEAM-PLASMA INSTABILITY IN MAGNETIZED PLASMAS

The minimal electromagnetic theory accommodating the axion-photon coupling can be constructed as follows ($\hbar = c = 1$) [45,46]:

$$\mathcal{L} = -\frac{1}{4}F_{\mu\nu}F^{\mu\nu} - A_\mu J_e^\mu + \mathcal{L}_\varphi + \mathcal{L}_{\text{int}}, \tag{1}$$

where $F_{\mu\nu} = \partial_\mu A_\nu - \partial_\nu A_\mu$ is the electromagnetic (EM) tensor, J_e^μ is the electron four-current, and $\mathcal{L}_\varphi = \partial_\mu\varphi^*\partial^\mu\varphi - m_\varphi^2|\varphi|^2$ is the axion Lagrangian (with φ denoting the axion field). For the QCD axion, $m_\varphi = \sqrt{z}f_\pi m_\pi/f_\varphi$, where $z = m_u/m_d$ is the up/down mass ratio, and $f_{\varphi(\pi)}$ is the axion (pion) decay constant [5,6]. Upon integration of the anomalous axion-gluon triangle, one obtains $\mathcal{L}_{\text{int}} = -(g/4)F_{\mu\nu}\tilde{F}^{\mu\nu}$, where $\tilde{F}^{\mu\nu} = \epsilon^{\mu\nu\alpha\beta}F_{\alpha\beta}$ denotes the dual EM tensor, and g is the axion-photon coupling. Although motivated for the QCD axion, the remainder of the paper is valid for any ALP. From Euler-Lagrange equations, one obtains Maxwell's equations [43], in particular, the Poisson equation

$$\nabla\cdot(\mathbf{E} + g\varphi\mathbf{B}) = \rho, \tag{2}$$

and the Klein-Gordon equation describing the axion field

$$(\Box + m_\varphi^2)\varphi = g\mathbf{E}\cdot\mathbf{B}, \tag{3}$$

with $\Box = \partial_t^2 - \nabla^2$ denoting the d'Alembert operator. In the situation of an electron beam propagating inside the plasma, $\rho = e(n_i - n_e - n_b)$, where n_i, n_e, and n_b, respectively, represent the ion, electron, and beam densities. As we are interested in electron plasma waves only, we can assume the ions to be immobile. Thus, the equations governing the dynamics of the plasma and beam electrons are given by

$$\frac{\partial n_\alpha}{\partial t} + \nabla\cdot(n_\alpha\mathbf{u}_\alpha) = 0, \tag{4}$$

with $\alpha = \{e, b\}$, and

$$\left(\frac{\partial}{\partial t} + \mathbf{u}_\alpha\cdot\nabla\right)\gamma_\alpha\mathbf{u}_\alpha = -\frac{e}{m_e}(\mathbf{E} + \mathbf{u}\times\mathbf{B}), \tag{5}$$

where $\gamma_\alpha = (1 - u_\alpha^2)^{-1/2}$ is the Lorentz factor. In the following, we will consider the plasma electrons to be initially at rest ($\gamma_e \simeq 1$), while the beam electrons propagate with velocity $\mathbf{u}_0$. We are interested in describing the electrostatic perturbations along a static, homogeneous magnetic field $\mathbf{B} = B_0\mathbf{e}_z$. As such, owing to the quasineutrality condition of the plasma, we perturb the densities as $n_e = n_0 + \tilde{n}_e$ and $n_b = fn_0 + \tilde{n}_b$ (here, f is the ratio of the beam to the plasma electrons), and the axion field as $\varphi = \tilde{\varphi}$ (neglecting the presence of a vacuum expectation value $\varphi_0 = 0$) to obtain

$$\begin{aligned}
&\frac{\partial^2}{\partial t^2}\tilde{n}_e - \frac{en_0}{m_e}\frac{\partial E}{\partial z} = 0,\\
&\left(\frac{\partial}{\partial t} + u_0\frac{\partial}{\partial z}\right)^2\tilde{n}_b - \frac{f}{\gamma_0^3}\frac{en_0}{m_e}\frac{\partial E}{\partial z} = 0,\\
&\left(\frac{\partial^2}{\partial t^2} - \nabla^2 + m_\varphi^2\right)\frac{\partial\tilde{\varphi}}{\partial z} - gB_0\frac{\partial E}{\partial z} = 0.
\end{aligned} \tag{6}$$

After Fourier transforming, this allows us to write Eq. (2) as $ik[\epsilon(k,\omega)E] = 0$, where

$$\epsilon(k,\omega) = 1 - \frac{\omega_p^2}{\omega^2} - \frac{f}{\gamma_0^3}\frac{\omega_p^2}{(\omega - ku_0)^2} - \frac{\Omega^4}{\omega^2(\omega^2-\omega_\varphi^2)} - \frac{f}{\gamma_0^3}\frac{\Omega^4}{(\omega-ku_0)^2(\omega^2-\omega_\varphi^2)} \tag{7}$$

is the dielectric permittivity, $\omega_p = \sqrt{e^2 n_0/(m_e)}$ is the plasma frequency, and $\omega_\varphi^2 = M_\varphi^2 + k^2$, with $M_\varphi = \sqrt{m_\varphi^2 + g^2 B_0^2}$ being the axion effective mass in the plasma. Here,

$$\Omega = \sqrt{gB_0\omega_p} \sim 2\pi \times (1.2\ \mathrm{Hz})\sqrt{\frac{g\times 10^{13}}{\mathrm{GeV}^{-1}}\frac{B_0}{\mathrm{T}}\frac{\omega_p}{\mathrm{GHz}}} \tag{8}$$

is the axion-plasmon coupling parameter (Rabi frequency). In the absence of the beam ($f = 0$), Eq. (7) yields the lower (L) and upper (U) polariton modes [43]

$$\omega_{\mathrm{L(U)}}^2 = \frac{1}{2}(\omega_\varphi^2 + \omega_p^2 \mp \sqrt{(\omega_\varphi^2 - \omega_p^2)^2 + 4\Omega^4}). \tag{9}$$

Conversely, in the absence of axions, Eq. (7) describes the celebrated beam-plasma instability [41,47]. For modes satisfying the condition $k \le k_c$, with

$$k_c = \frac{\omega_p}{u_0}(1+\nu^{1/3})^{3/2}, \qquad (\nu = f/\gamma_0^3) \tag{10}$$

being the cutoff wave vector, the plasma and the beam (with dispersion $\omega = \sqrt{\nu}\omega_p + u_0 k$) modes coalesce, and the resulting dispersion relation becomes complex. In the unstable region, the dispersion relation of the plasma reads $\omega \simeq \omega_r + i\gamma_p$, where $\omega_r = u_0 k(1-\nu^{2/3})$, and γ_p is the instability growth rate [41,47]

$$\gamma_p = \frac{\nu^{2/3}}{\sqrt{3}(1+\nu^{4/3})^{5/2}}\frac{u_0^2 k^2}{\omega_p}\left[\frac{\omega_p^2}{u_0^2k^2}(1+\nu^{4/3})^3 - 1\right]^{1/2}. \tag{11}$$

The most unstable mode occurring at $k \simeq \omega_p/u_0$ grows at the rate $\gamma_p^{\max} \simeq 0.69\nu^{2/3}\omega_p$. These features are depicted in Fig. 2(a).

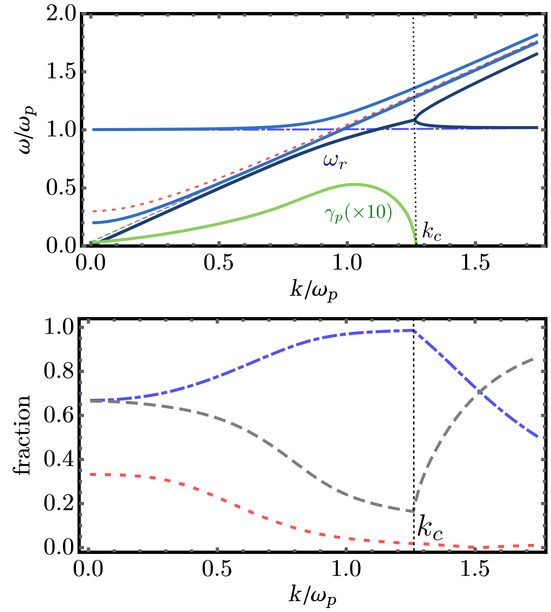

FIG. 2. Top panel: Dispersion relation of the axion-plasmon polariton in the streaming instability situation. The dashed lines are the bare dispersions. Axion (red/dotted line), plasmon (blue/dot-dashed line), and electron beam (gray/dashed line). The black solid lines depict the real part of the modes, while the green line represents the imaginary part of the coalesced plasma-beam mode. For illustration, we have set $f = 0.2$, $m_\varphi = 0.3\omega_p$, $u_0 = 0.97$, and the exaggerated value $\Omega = 0.1\omega_p$. Bottom panel: The axion (red/dotted), plasma (blue/dot-dashed), and beam (gray/dashed) fractions in the unstable mode, as obtained by extracting the eigenvalues of Eq. (6).

III. PLASMON-AXION CONVERSION

Given the smallness of Ω, the instability does not change noticeably in the perspective of the plasma, and therefore, the discussion above holds even in the presence of axions. However, and more crucially, the small fraction of axion that participates in the beam-plasma dynamics leads to the production of axions. The fractions (i.e., the eigenvectors) can be determined by solving the eigenvalue problem in Eq. (6) numerically, as illustrated in Fig. 2(b). The axion production mechanism can thus be understood as follows: The beam transfers energy to the plasma, which becomes unstable; then, the magnetic field mixes the axion and the plasmon modes, allowing the latter to be converted into the former. To estimate this, we notice that the coupling between the axion and the plasma is much larger than that with the beam, resulting in the separation of scales $\omega_p^2 \gg \Omega^2 \gg \nu\Omega^2$. Under this conditions, we can solve Eqs. (6) numerically to compute the plasmon-axion conversion probability in the beam-plasma configuration. In the quasilinear diffusion regime, allowing us to accommodate the instability saturation by substituting $\gamma_p \to \gamma_p[1 - 9\omega_p^4 n(t)^2/(8\gamma_p^4 n_0^2)]$ in the eigenvalue problem [48,49], we obtain the following piecewise function (see [50] for details)

$$P_{p\to\varphi} = \begin{cases} e^{2\gamma_p t} P_{p\to\varphi}^{\mathrm{osc}}, & t \le \tau_{\mathrm{sat}}, \\ e^{2\gamma_p \tau_{\mathrm{sat}}} P_{p\to\varphi}^{\mathrm{osc}}, & t > \tau_{\mathrm{sat}}, \end{cases} \tag{12}$$

where $\tau_{\mathrm{sat}} \sim \nu^{-1/3}\omega_p/\gamma_p^2$ is the typical beam-plasma instability saturation time. Here,

$$P_{p\to\varphi}^{\mathrm{osc}} = \frac{g^2 B_0^2 \sin^2\left[\frac{t}{2}\sqrt{g^2B_0^2 - (\omega_r - \omega_\varphi)^2}\right]}{4[g^2B_0^2 - (\omega_r-\omega_\varphi)^2 - \gamma_p^2]} \tag{13}$$

is the oscillating probability in the plasma [50]. For a discharge plasma column of size $L \sim 3.15$ m and plasma frequency $\omega_p \sim 2\pi \times 1$ GHz in a magnetic field of $B_0 \sim 1$ T, with a growth rate of $\gamma_p \sim 10^{-2}\omega_p$ at resonance, and taking $g \sim 10^{-13}$ GeV^{-1}, we obtain $P_{p\to\varphi} \sim 10^{-21}$ for the most unstable mode, $k \sim \omega_p/u_0$. This happens for sufficiently light axions $m_\varphi \lesssim 0.1\omega_p \simeq 0.4$ μeV, for which $\tau_{\rm flight} < \tau_{\rm sat}$, where $\tau_{\rm flight} = L/v_\varphi$ (with $v_\varphi = \partial_k\omega_\varphi$) denotes the axion time of flight in a plasma column of size L. For higher values of the mass, $\tau_{\rm flight} > \tau_{\rm sat}$, and the saturation probability can go up to 10^{-16}, deep in the saturation regime [50]. This remarkable enhancement of the conversion probability is a consequence of the significant electric field produced by the instability.

The axions resulting from the PSW experiment above can then be sent into a regeneration chamber and be eventually converted into photons, similar to what is done in the LSW schemes [23]. For that task, we consider a homogeneous, transverse magnetic field $\mathbf{B}_\perp$ in a cavity of length d, for which the corresponding axion-photon conversion rate is given by $P_{\varphi\to\gamma} \simeq \sin^2\Theta\sin^2(\Delta k d)$, where $\tan(\Theta) = gB_0\omega/(m_\varphi^2 - m_\gamma^2)$ is the mixing angle and $\Delta k = |\sqrt{\omega^2 - m_\varphi^2} - \sqrt{\omega^2 - m_\gamma^2}|$ is the axion-photon momentum difference, and m_γ is the photon mass in the buffer gas [28]. To estimate the order of magnitude of the photon flux at the detector, we relate the energy $\mathcal{E}$ delivered in the plasma by an electron beam of energy E_b and density fn_0 to the number of plasmons created, i.e., $\mathcal{E}/V = fn_0E_b = N_p\omega_p/V = N_\varphi\omega_p/(VP_{p\to\varphi})$, with $N_{p(\varphi)}$ denoting the average number of plasmons (axions). Assuming that the beams can be injected in a plasma at the repetition rate R_b, we obtain the photon power per volume as [8]

$$\frac{P}{V} \simeq R_b\frac{\omega_\varphi}{\omega_p}fn_0E_b\mathcal{Q}\mathcal{G}P_{p\to\varphi}P_{\varphi\to\gamma}, \tag{14}$$

where $\mathcal{Q} = \mathcal{Q}_\varphi\mathcal{Q}_c/(\mathcal{Q}_\varphi + \mathcal{Q}_c)$ is the reduced cavity quality factor [51] (depending on the produced axion $\mathcal{Q}_\varphi \sim \omega_p/\gamma_p \simeq 10^2$ and on the cavity $\mathcal{Q}_c$ quality factors) and $\mathcal{G}$ is the cavity form factor. The signal-to-noise ratio S/N can then be determined using Dicke's radiometer equation [52]

$$S/N = \frac{P}{T_{\rm noise}}\sqrt{\frac{2\pi\tau}{\Delta\omega}}, \tag{15}$$

where $T_{\rm noise}$ is the system noise temperature, $\Delta\omega \simeq \mathcal{Q}_c^{-1}$ is the bandwidth, and τ is the scanning time. For the conditions discussed above, and assuming a magnetic field of $B_\perp = 10$ T to be homogeneous in a cavity of length $d = 10$ m [23,53], we expect a state-of-the-art linear amplifier (considering moderate values, $\mathcal{Q}_c \simeq 10^5$ and $\mathcal{G} \simeq 0.65$ [53]) operating with a high electron mobility transistor cooled with liquid helium (we use $T_{\rm noise} \sim 5$ K, above the quantum limit [40]) to be sensitive to resonant axions $\omega_\varphi \sim \omega_p$ in the region $g \sim 10^{-12}$ GeV^{-1}. For this order-of-magnitude

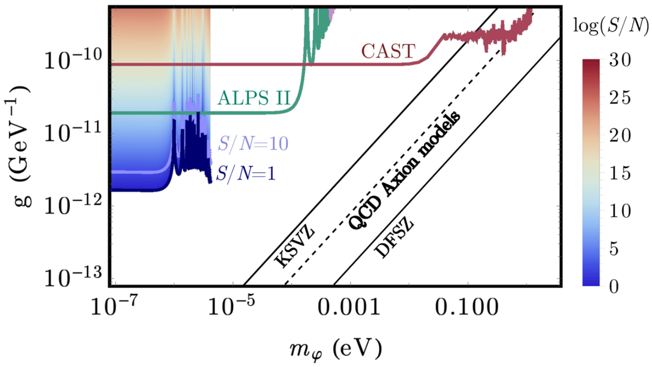

FIG. 3. Sensitivity of a plasma-shinning-through-a-wall experiment based on a linear amplifier detection, computed for a regeneration path of $d = 10$ m in a transverse magnetic field $B_\perp = 10$ T. We have considered a 1 m^3 plasma in a cylindrical column of $L = 3.15$ m with plasma frequency $\omega_p = 2\pi \times 1$ GHz in $B_0 = 1$ T magnetic field. The electron beam concentration is $f = 3.4$, with an energy of $E_b = 3.0$ MeV and a repetition rate $R_b = 100$ Hz. The sensitivities of the CAST [17] and Bhre *et al.* experiments [24] are also depicted for comparison.

estimate, we take a scanning time of $\tau = 100$ h and require a reasonable signal-to-noise ratio of $S/N = 10$ (see Fig. 3). Our results suggest that the proposed PSW scheme may compete with the performance of current LSW experiments, such as Bhre *et al.* [24], in a narrow gap of axion masses. We have considered the case $m_\gamma = 0$ (no buffer), but the sensitivity can be further improved by introducing a buffer gas in the regeneration chamber, or by increasing the magnetic field B_0 in the plasma (production) chamber. At this stage, however, we are mainly focused on the order-of-magnitude estimate rather than an exhaustive design of the experimental setup. Moreover, by increasing the plasma frequency close to tens of GHz, single-photon microwave technology may be possibly used to project PSW setups in future investigations. [54,55].

Our findings can also be interesting to identify signatures of axion production via plasma instabilities taking place in magnetar magnetic pole caps. As it is known, alongside with the gamma-ray emission taking place in the region of high-density, boosted plasma [56], the beam-plasma instability leads to the formation of plasma bunches that generate radio emission via the curvature effect [57,58]. During this process, the produced axions may be resonantly converted into photons at the radius r_c related to the Goldreich-Julian magnetosphere density [59,60]

$$n_c = \frac{2\pi B_0}{eP}\frac{1}{1 - 4\pi^2r_c^2\sin^2\theta/P}, \tag{16}$$

where P is the pulsar period, and θ is the polar angle with respect to the rotation axis. For $\theta = 90°$, the corresponding plasma frequency is $\omega_p/2\pi \simeq (1.5 \times 10^2\ \mathrm{GHz})\sqrt{(B/10^{14}\ \mathrm{G})(1\ \mathrm{sec}/P)}$ yielding $\omega_p \sim 2\pi \times 98$ GHz for the SGR J145-2900 magnetar ($P \simeq 3.76$ s,

$B_0 \simeq 1.6 \times 10^{14}$ G [61,62]), a value not too far from the discharge plasma discussed above. There are two electromagnetic modes propagating in a transverse magnetic field: the ordinary (the O) mode, with parallel polarization $\mathbf{E} \parallel \mathbf{B}_0$, and the extraordinary (the X) mode, of perpendicular polarization $\mathbf{E} \perp \mathbf{B}_0$ [41]. From Eq. (3), it is clear that only the former can result from the axion-photon decay process and satisfies the dispersion relation $\omega^2 = \omega_p^2 + k^2$. Since only photons with frequency larger than the ω_p escape the plasma, and given that the plasma instability terminates at the cutoff frequency $\omega_c = \sqrt{m_\varphi^2 + k_c^2}$, axion-photon conversion will occur in the range $\omega_p \leq \omega \leq \omega_c$. For resonant conversion $\omega_p \simeq m_\varphi$, the cutoff frequency reads

$$\omega_c = \sqrt{m_\varphi^2 + k_c^2} \simeq \sqrt{2}\omega_p \left[1 + \frac{3}{4} f^{1/3} \frac{m_e}{E_b}\right] \tag{17}$$

valid for relativistic electron beams, $E_b \gg m_e$. Assuming the electron beam to be much more energetic than the electron-positron plasma (making the cold plasma model valid), and taking a beam relativistic factor of $\gamma_0 \sim 10^6$, we estimate a cutoff frequency of $\omega_c \simeq 2\pi \times 137$ GHz. As such, a signal in the range 98 GHz $\leq \omega/2\pi \leq$ 137 GHz might be expected for the conditions of the experiment proposed in Refs. [38,63] based on axion dark matter conversion (notice that in our case we do not need a dark matter background). At this stage, however, we cannot confirm whether or not the axions produced via streaming instability can be detected within the sensitivity of telescopes such as CAST or the Arecibo Telescope for the typical observation periods (this would involve a more detailed calculation of the beam injection rates, intensity, energies, etc.), but we anticipate that the narrow spectrum in Eq. (17) would be a clear signature of this process.

IV. CONCLUSION

We have shown that a magnetized plasma can be an active source of axions and axionlike particles. For that, we have exploited the beam-stream instability triggered by a monoenergetic electron beam to convert plasmons into axions. The production mechanism is based on the transfer of energy from the electrons to the small axion-plasmon admixture, the latter being a consequence of the axion-plasmon polariton coupling occurring in magnetized plasmas [43]. An estimation of the sequent conversion of the axion into a photon in a transverse magnetic field suggests that our schemes can compete with some of the existing light-shining-through-a-wall experiments such as OSQAR [25], Redondo and Ringwald [64], and Ehret *et al.* [65]. The present scheme differs from other plasma-based setup, such as that proposed in Ref. [33], in several aspects: (i) The gain mechanism is enhanced via a plasma instability, (ii) we do not require a petawatt laser facility to achieve reasonable conversion probabilities, making it easier to couple with a regeneration cavity, and (iii) our repetition rates are, at least, 1 order of magnitude higher. Most likely, our findings will motivate the design of plasma-shining-a-wall setups for tunable ranges of axion masses in the near future, especially when combined with plasma metamaterials as in Ref. [40]. Moreover, given the abundance of astrophysical bodies displaying beam-plasma and beam-beam instabilities, we anticipate that a plethora of new exciting phenomena involving the dynamics of axions in plasma may arise, adding a new twist to the phenomenology of axions and axionlike particles in astrophysics [37–39,66–69].

ACKNOWLEDGMENTS

The authors acknowledge Fundação da Ciência e Tecnologia (FCT-Portugal) through the Grant No. IF/00433/2015.

[1] J. M. Pendlebury, S. Afach, and N. J. Ayres *et al.* Phys. Rev. D **92**, 092003 (2015).
[2] J. Jaeckel and A. Ringwald, Annu. Rev. Nucl. Part. Sci. **60**, 405 (2010).
[3] A. Ringwald, Phys. Dark Universe **1**, 116 (2012).
[4] J. E. Kim and G. Carosi, Rev. Mod. Phys. **82**, 557 (2010).
[5] R. D. Peccei and H. R. Quinn, Phys. Rev. Lett. **38**, 1440 (1977).
[6] S. Weinberg, Phys. Rev. Lett. **40**, 223 (1978).
[7] F. Wilczek, Phys. Rev. Lett. **40**, 279 (1978).
[8] P. Sikivie, Phys. Rev. Lett. **51**, 1415 (1983).
[9] S. J. Asztalos, G. Carosi, C. Hagmann, D. Kinion, K. van Bibber, M. Hotz, L. J. Rosenberg, G. Rybka, J. Hoskins, J. Hwang, P. Sikivie, D. B. Tanner, R. Bradley, and J. Clarke, Phys. Rev. Lett. **104**, 041301 (2010).
[10] M. I. Vysotsky, Y. B. Zeldovich, M. Y. Khlopov, and V. M. Chechetkin, Pis'ma Zh. Eksp. Teor. Fiz. **27**, 533 (1978) [JETP Lett. **27**, 502 (1978)].
[11] Z. G. Berezhiani, M. Y. Khlopov, and R. R. Khomeriki, Yad. Fiz. **52**, 104 (1990) [Sov. J. Nucl. Phys. **52**, 65 (1990)].
[12] M. Khlopov, A. Sakharov, and D. Sokoloff, Nucl. Phys. B, Proc. Suppl. **72**, 105 (1999).
[13] K. Zioutas *et al.* (CAST Collaboration), Phys. Rev. Lett. **94**, 121301 (2005).
[14] M. Fairbairn, T. Rashba, and S. Troitsky, Phys. Rev. Lett. **98**, 201801 (2007).
[15] P. Gondolo and L. Visinelli, Phys. Rev. Lett. **113**, 011802 (2014).

[16] D. S. Akerib *et al.* (LUX Collaboration), Phys. Rev. Lett. **118**, 261301 (2017).
[17] CAST Collaboration, Nat. Phys. **13**, 584 (2017).
[18] S. Asztalos, E. Daw, H. Peng, L. J. Rosenberg, C. Hagmann, D. Kinion, W. Stoeffl, K. van Bibber, P. Sikivie, N. S. Sullivan, D. B. Tanner, F. Nezrick, M. S. Turner, D. M. Moltz, J. Powell, M.-O. André, J. Clarke, M. Mück, and R. F. Bradley, Phys. Rev. D **64**, 092003 (2001).
[19] S. J. Asztalos, G. Carosi, C. Hagmann, D. Kinion, K. van Bibber, M. Hotz, L. J. Rosenberg, G. Rybka, J. Hoskins, J. Hwang, P. Sikivie, D. B. Tanner, R. Bradley, and J. Clarke, Phys. Rev. Lett. **104**, 041301 (2010).
[20] N. Du *et al.* (ADMX Collaboration), Phys. Rev. Lett. **120**, 151301 (2018).
[21] J. K. Vogel *et al.*, Phys. Procedia **61**, 193 (2015).
[22] A. Caldwell, G. Dvali, B. Majorovits, A. Millar, G. Raffelt, J. Redondo, O. Reimann, F. Simon, and F. Steffen (MADMAX Working Group), Phys. Rev. Lett. **118**, 091801 (2017).
[23] F. Januschek, in *Proceedings of the 10th Patras Workshop on Axions, WIMPs and WISPs, AXION-WIMP 2014, Geneva, Switzerland* (Verlag Deutsches Elektronen-Synchrotron, Hamburg, 2014), pp. 83–88.
[24] R. Bähre, B. Döbrich, J. Dreyling-Eschweiler, S. Ghazaryan, R. Hodajerdi, D. Horns, F. Januschek, E. A. Knabbe, A. Lindner, D. Notz, A. Ringwald, J. E. von Seggern, R. Stromhagen, D. Trines, and B. Willke, J. Instrum. **8**, T09001 (2013).
[25] P. Pugnat, L. Duvillaret, R. Jost, G. Vitrant, D. Romanini, A. Siemko, R. Ballou, B. Barbara, M. Finger, M. Finger, J. Hošek, M. Král, K. A. Meissner, M. Šulc, and J. Zicha (OSQAR Collaboration), Phys. Rev. D **78**, 092003 (2008).
[26] L. Capparelli, G. Cavoto, J. Ferretti, F. Giazotto, A. Polosa, and P. Spagnolo, Phys. Dark Universe **12**, 37 (2016).
[27] M. Betz, F. Caspers, M. Gasior, M. Thumm, and S. W. Rieger, Phys. Rev. D **88**, 075014 (2013).
[28] G. Raffelt and L. Stodolsky, Phys. Rev. D **37**, 1237 (1988).
[29] S. Mangles, C. Murphy, Z. Najmudin, A. Thomas, J. Collier, A. Dangor, E. Divall, P. Foster, J. Gallacher, C. Hooker, D. Jaroszynski, A. Langley, W. Mori, P. Norreys, F. Tsung, R. Viskup, B. Walton, and K. Krushelnick, Nature (London) **431**, 535 (2004).
[30] C. G. R. Geddes, C. Toth, J. van Tilborg, E. Esarey, C. B. Schroeder, D. Bruhwiler, C. Nieter, J. Cary, and W. P. Leemans, Nature (London) **431**, 538 (2004).
[31] J. Faure, Y. Glinec, A. Pukhov, S. Kiselev, S. Gordienko, E. Lefebvre, J.-P. Rousseau, F. Burgy, and V. Malka, Nature (London) **431**, 541 (2004).
[32] E. Adli *et al.*, Nature (London) **561**, 363 (2018).
[33] D. A. Burton and A. Noble, New J. Phys. **20**, 033022 (2018).
[34] D. A. Burton and A. Noble, J. Phys. A **43**, 075502 (2010).
[35] D. A. Burton, A. Noble, and T. J. Walton, J. Phys. A **49**, 385501 (2016).
[36] J. T. Mendonça, Europhys. Lett. **79**, 21001 (2007).
[37] M. S. Pshirkov and S. B. Popov, J. Exp. Theor. Phys. **108**, 384 (2009).
[38] A. Hook, Y. Kahn, B. R. Safdi, and Z. Sun, Phys. Rev. Lett. **121**, 241102 (2018).
[39] S. Sen, Phys. Rev. D **98**, 103012 (2018).
[40] M. Lawson, A. J. Millar, M. Pancaldi, E. Vitagliano, and F. Wilczek, Phys. Rev. Lett. **123**, 141802 (2019).
[41] F. F. Chen, *Introduction to Plasma Physics* (Springer, New York, 2012).
[42] E. Asseo, R. Pellat, and M. Rosado, Astrophys. J. **239**, 661 (1980).
[43] H. Terças, J. D. Rodrigues, and J. T. Mendonça, Phys. Rev. Lett. **120**, 181803 (2018).
[44] S. Das, P. Jain, J. P. Ralston, and R. Saha, Pramana **70**, 439 (2008).
[45] L. Visinelli, Mod. Phys. Lett. A **28**, 1350162 (2013).
[46] F. Wilczek, Phys. Rev. Lett. **58**, 1799 (1987).
[47] D. Anderson, R. Fedele, and M. Lisak, Am. J. Phys. **69**, 1262 (2001).
[48] T. M. O'Neil, J. H. Winfrey, and J. H. Malmberg, Phys. Fluids **14**, 1204 (1971).
[49] A. S. Sharma and B. Buti, Pramana **6**, 329 (1976).
[50] See Supplemental Material at http://link.aps.org/supplemental/10.1103/PhysRevD.101.051701 for details on the calculation of the plasmon-axion conversion probability, Eq. (12).
[51] D. Kim, J. Jeong, S. Youn, Y. Kim, and Y. K. Semertzidis, arXiv:2001.05605.
[52] R. H. Dicke, Rev. Sci. Instrum. **17**, 268 (1946).
[53] O. K. Baker, M. Betz, F. Caspers, J. Jaeckel, A. Lindner, A. Ringwald, Y. Semertzidis, P. Sikivie, and K. Zioutas, Phys. Rev. D **85**, 035018 (2012).
[54] S. K. Lamoreaux, K. A. van Bibber, K. W. Lehnert, and G. Carosi, Phys. Rev. D **88**, 035020 (2013).
[55] K. Inomata, Z. Lin, K. Koshino, W. D. Oliver, J.-S. Tsai, T. Yamamoto, and Y. Nakamura, Nat. Commun. **7**, 12303 (2016).
[56] Although the beam-plasma instability also occurs for high-density plasmas, the produced axions would not decay into photons resonantly, as the plasma frequency largely exceeds the axion masses predicted by the models.
[57] Y. P. Ochelkov and V. V. Usov, Nature (London) **309**, 332 (1984).
[58] M. A. Ruderman and P. G. Sutherland, Astrophys. J. **196**, 51 (1975).
[59] P. Goldreich and W. H. Julian, Astrophys. J. **157**, 869 (1969).
[60] D. B. Melrose and R. Yuen, J. Plasma Phys. **82**, 635820202 (2016).
[61] J. A. Kennea, D. N. Burrows, C. Kouveliotou, D. M. Palmer, E. Gögüs, Y. Kaneko, P. A. Evans, N. Degenaar, M. T. Reynolds, J. M. Miller, R. Wijnands, K. Mori, and N. Gehrels, Astrophys. J. Lett. **770**, L24 (2013).
[62] R. P. Eatough *et al.* Nature (London) **501**, 391 (2013).
[63] F. P. Huang, K. Kadota, T. Sekiguchi, and H. Tashiro, Phys. Rev. D **97**, 123001 (2018).
[64] J. Redondo and A. Ringwald, Contemp. Phys. **52**, 211 (2011).
[65] K. Ehret, M. Frede, S. Ghazaryan, M. Hildebrandt, E.-A. Knabbe, D. Kracht, A. Lindner, J. List, T. Meier, N. Meyer, D. Notz, J. Redondo, A. Ringwald, G. Wiedemann, and B. Willke, Phys. Lett. B **689**, 149 (2010).
[66] A. S. Sakharov and M. Y. Khlopov, Yad. Fiz. **57**, 514 (1994) [Phys. At. Nucl. **57**, 485 (1994)].
[67] A. De Angelis, M. Roncadelli, and O. Mansutti, Phys. Rev. D **76**, 121301 (2007).
[68] F. Tavecchio, M. Roncadelli, G. Galanti, and G. Bonnoli, Phys. Rev. D **86**, 085036 (2012).
[69] G. Galanti and M. Roncadelli, J. High Energy Astrophys. **20**, 1 (2018).